Theoretical study of CH 4 photodissociation on the Pt(111) surface

Yoshinobu Akinaga, Tetsuya Taketsugu, and Kimihiko Hirao

Citation: The Journal of Chemical Physics **107**, 415 (1997); doi: 10.1063/1.474403
View online: http://dx.doi.org/10.1063/1.474403
View Table of Contents: http://scitation.aip.org/content/aip/journal/jcp/107/2?ver=pdfcov
Published by the AIP Publishing

Theoretical study of CH_4 photodissociation on the Pt(111) surface

Yoshinobu Akinaga, Tetsuya Taketsugu, and Kimihiko Hirao
Department of Applied Chemistry, Graduate School of Engineering, University of Tokyo, Tokyo 113, Japan

(Received 12 February 1997; accepted 4 April 1997)

The photodissociation of CH_4/Pt(111) is studied by density functional theory and the state-averaged complete active space self-consistent field (SA-CASSCF) method using a cluster model Pt_n ($n=1,4,6,7,10$). With the small clusters ($n \leqslant 4$), the equilibrium molecule–surface distances (H_3CH–Pt) are less than 2.3 Å and the binding energies are 4–14 kcal/mol, the order of the chemisorption. With larger clusters, the molecule–surface distance and the binding energy are calculated to be 3.00 Å and 0.67 kcal/mol, respectively, of the order of the physisorption, which coincides with the experiments. The SA-CASSCF calculations verify that, in spite of the weak interaction between CH_4 and Pt_n in the ground state, the first excited state of CH_4 (Rydberg type) interacts with Pt_n unoccupied states strongly, resulting in the charge-transfer state and finally leading to the dissociation to $CH_3+H(-Pt)$; on the Pt(111) surface, the excitation energy to the Rydberg state of CH_4 decreases by ~ 3 eV compared to that in an isolated CH_4 molecule. These results support the experimental results that the direct excitation of CH_4 is invoked on the Pt(111) surface by irradiation of the 193 nm photon, leading to the dissociation to CH_3 and H. © *1997 American Institute of Physics.* [S0021-9606(97)02326-X]

I. INTRODUCTION

Recently, many investigations have been done on surface photochemistry, e.g., photostimulated desorption and photodissociation on the transition metal surface.[1] In surface photochemistry, electronic excited states of an adsorbate–substrate system play an important role, so theoretical approaches may offer great advantages. For example, Nakatsuji *et al.*[2] studied the photostimulated desorption of CO from a Pt surface by the symmetry adapted cluster (SAC) and SAC-CI (configuration-interaction) methods[3] using a cluster model including an image force correction,[4] and classified several excitation types leading to desorption.

The mechanism of electronic excitation of adsorbed molecules on a solid surface is classified into two types; a direct excitation of adsorbate (or adsorbate–substrate complex) and a surface-mediated electron attachment.[1] In the former, the photon absorption is localized at adsorbate or, when the molecule–surface interaction is strong, at the adsorbate–substrate complex (e.g., in the dielectric or semiconductor surface). In the surface-mediated mechanism, a hot electron created via photon absorption on the surface is transferred to adsorbed molecules, which become a transient negative ion state leading to the reaction. Ho *et al.*[5] reported that, in the photodissociation of $Mo(CO)_6$ physisorbed on various surfaces, the direct excitation of adsorbed molecules is a major process. In a phosgene (Cl_2CO) case, it was reported[6] that both the direct excitation and the surface-mediated excitation occur. In these cases, excited states of the adsorbate are little perturbed by surfaces.

Recently, Matsumoto *et al.*[7–9] reported that CH_4 physisorbed on a Pt(111) surface is dissociated into a hydrogen atom and a methyl radical upon irradiation with a 193 nm (6.43 eV) photon under ultrahigh vacuum condition. Note that gas phase CH_4 shows continuous absorption spectra in the region of <145 nm (8.56 eV photon).[10,11] They measured the polarization-dependent photochemical cross section as a function of the incident angle, and concluded that the direct excitation of adsorbed methane plays an essential role in the dissociation of methane on the Pt(111) surface. Since CH_4 interacts very weakly with a Pt surface (~ 0.23 eV adsorption energy),[9] the shift of excitation energy of ~ 2 eV is remarkable and mysterious if the direct excitation actually takes place.

The purpose of the present study is to clarify the mechanism of excitation of methane physisorbed on the Pt(111) surface. We used a cluster model, and calculated the adsorption structure as well as the electronic structures of ground and several excited states of CH_4–Pt_n systems by the density functional theory (DFT)-based method, B3LYP with Becke's 3 parameter functional using the Lee–Yang–Parr nonlocal correlation functional,[12–14] and the complete active space self-consistent field (CASSCF) method.[15]

II. COMPUTATIONAL DETAIL

A Pt(111) surface was represented by a cluster model, Pt_n ($n=1,4,6,7,10$). Yoshinobu *et al.*[6] reported that CH_4 physisorbed on the Pt(111) surface has C_{3v} or lower symmetry by means of infrared reflection absorption spectroscopy (IRAS). So, we carried out geometry optimizations by DFT with B3LYP[12–14] for the CH_4 (T_d symmetry) and CH_4–Pt_n systems (C_{3v} symmetry) shown in Figs. 1(a) and 1(b), using the GAUSSIAN94 program.[17] Here, Pt–Pt distances are fixed at 2.7746 Å, which is the lattice distance of a Pt fcc crystal.[18] Figure 1(a) shows on-top structures of CH_4–Pt_n ($n=1,4,7,10$) in which one H atom is pointed directly at one Pt atom, while Fig. 1(b) shows the other type structures of CH_4–Pt_n ($n=6,7$). The electronic structures of the ground and several excited states for CH_4 and CH_4–Pt_n were calcu-

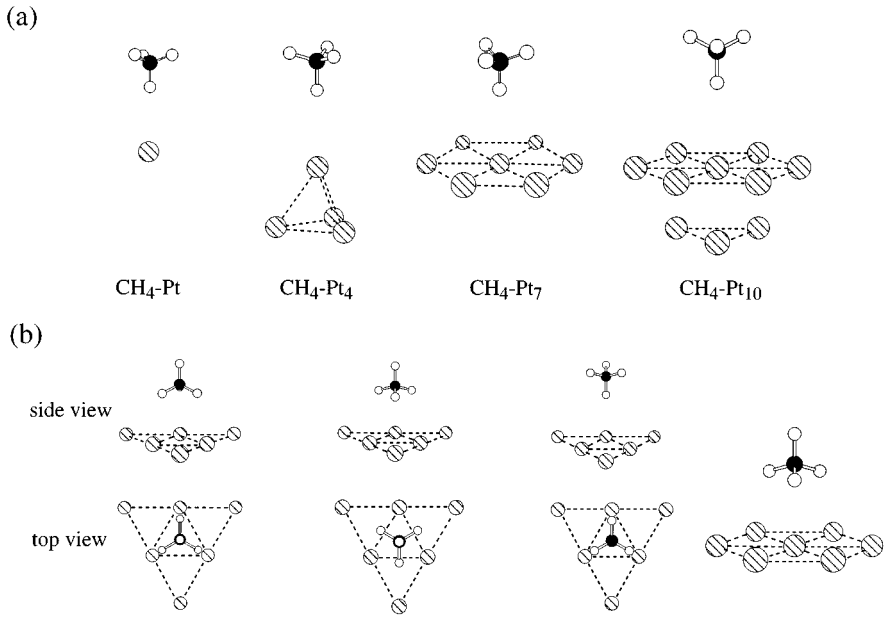

FIG. 1. CH_4–Pt_n adsorption structures with C_{3v} symmetry ($n=1,4,6,7,10$): (a) on-top type; (b) the other type.

lated by the state-averaged CASSCF (SA-CASSCF) method[15] with several different active spaces using the MOLPRO96 program.[19]

For C and H, Dunning's augmented cc-pVDZ basis sets[20] were used. For Pt, the Xe core was replaced by the relativistic effective core potential while the valence $5d$ and $6s$ electrons were treated explicitly by $(3s3p3d)/[2s2p2d]$ Gaussian basis functions.[21] The CASSCF with this basis set reproduces the Pt atomic energy splitting between $^3D(5d^96s^1)$ and $^1S(5d^{10}6s^0)$ to be 0.66 eV, which is compared to the experimental value of 0.75 eV. For CH_4–Pt_{10}, the $(3s3p3d)/[2s1p1d]$ basis set was used for nine Pt atoms which do not directly interact with CH_4.

III. RESULTS AND DISCUSSION

A. Adsorption structure

We first discuss the adsorption structures of CH_4–Pt_n systems optimized by the B3LYP method. With the small clusters, $n=1$ and 4, we considered only on-top structures [Fig. 1(a)]. In these systems, the H_{ad}–Pt distances (H_{ad} is the one closest to Pt) were calculated to be 2.07 and 2.29 Å, respectively, which are of the order of the chemisorption, and the adsorption energies are 3.5 and 14.1 kcal/mol, respectively. Note that the experimentally suggested H_{ad}–Pt distance is 2.6 Å, and the interaction between the CH_4 and Pt surface was reported to be as weak as the physisorption.[7–9] This result suggests that Pt and Pt_4 clusters are insufficient to represent a Pt(111) surface. As for the larger system, $n=6$ and 7, we examined five adsorption structures (on-top and the other four) shown in Fig. 1, but only the on-top structure ($n=7$) proved to be stable. The distance of H_{ad}–Pt was calculated to be 3.00 Å, which corresponds clearly to the physisorption. The adsorption energy is very small (~0.67 kcal/mol), implying the quite shallow minimum and the weak interaction between CH_4 and the Pt surface.

To examine the difference of the adsorption mechanism in CH_4–Pt_4 (chemisorption) and CH_4–Pt_7 (physisorption), the difference density maps for these systems are given in Fig. 2. The H_{ad}–Pt_{ad} distance is fixed at 2.29 Å, which is the optimized distance for CH_4–Pt_4. CH_4–Pt_4 is stabilized by 14.1 kcal/mol at this structure while CH_4–Pt_7 is unstable by 0.77 kcal/mol relative to their dissociation limit, CH_4+Pt_n. The charge redistributions are distinctly different in these two systems. In CH_4–Pt_4, the $H_3C\cdots H_{ad}$ density decreases while the $H_{ad}\cdots Pt_{ad}$ density increases, relative to the unperturbed CH_4 and Pt cluster, which is characteristic in the weak interaction such as the hydrogen bonding. The electron is donated from Pt $5d_{z^2}$ to the CH antibonding orbital. The charge transfer is essential but not significant. In CH_4–Pt_7, however, the $H_3C\cdots H_{ad}$ density increases while the $H_{ad}\cdots Pt_{ad}$ density decreases. This charge redistribution resembles that of the He···He repulsive interaction. This marked difference originates from the exchange repulsion, which should become greater as CH_4 approaches Pt_n. In CH_4–Pt_4, electrons in Pt $5d_{z^2}$ can easily polarize to avoid the exchange repulsion and CH_4 can come closer to interact with Pt. In CH_4–Pt_7, however, it is prohibited due to the crowded electron cloud of the neighboring Pt atoms, and the electron density in the region between H_{ad} and Pt decreases to avoid the exchange repulsion.

As to the ground state, the nature of the interaction is quite different between CH_4–Pt_4 and CH_4–Pt_7. The cluster model with a small number of Pt atoms cannot mimic the Pt surface. This implies that we need at least seven Pt atoms to model the Pt surface in the sense that it gives a physisorption structure coinciding with the experiment. (Of course, the

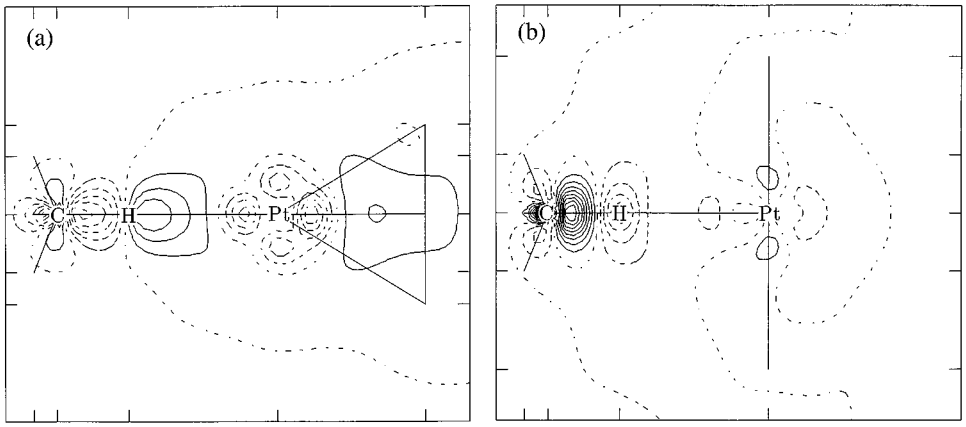

FIG. 2. The density difference maps for (a) CH_4–Pt_4 and (b) CH_4–Pt_7, with the H_{ad}–Pt_{ad} distance fixed at 2.29 Å. The full lines and the broken lines denote the increase and the decrease of the charge density relative to the separate noninteracting CH_4 and Pt_n, respectively.

very long bond length calculated for H_{ad}–Pt_{ad} means that the surface may still not be well described by Pt_7.) Although the ground state chemistry is different between small and large Pt clusters, there is no substantial difference in the excited states, which will be given later.

The structure of CH_4 adsorbed on Pt_7 is almost the same as that for isolated CH_4 (CH bond length: 1.100→1.097 (CH_{ad}), 1.095 (others) Å; HCH_{ad} bond angle: 109.47 →109.44 deg). In the following, we will consider only the on-top structures [Fig. 1(a)] and employ the CH_4–Pt_7 adsorption structure (CH_4 structure and H–Pt distance) for all the cluster models.

B. CH_4

The photodissociation of CH_4 has been studied by various experimental[10] and theoretical[22,23] methods. The gaseous methane shows a continuous absorption spectra beginning from 145 nm (8.56 eV photon) but the first-excited triply degenerate state $1\,^1T_2$ (Rydberg type) lies about 10 eV above the ground state, which is crossed by a valence antibonding state leading to the dissociation.[10] Absorption peaks at 9.7 and 10.3 eV originate from this excited state, of which degeneracy has been broken through the Jahn–Teller effect.[10] They dissociate into CH_2+H_2 and CH_3+H, respectively.

For the isolated CH_4, we performed a SA-CASSCF calculation averaging the ground and triply degenerate excited states ($1t_2 \rightarrow 3a_1$) at the B3LYP optimized structure. As the active space, eight valence orbitals and a C $3s$ Rydberg orbital were included [eight electrons in nine orbitals: (8/9)]. The excitation energy is calculated as 10.16 eV, which is in good agreement with the experimental value. To check the validity of the active space, we also performed the SA-CASSCF(8/12) calculation, adding C $3p$ Rydberg orbitals to the active space, and obtained almost the same value (10.16 eV).

C. CH_4–Pt

1. Ground and excited states at the adsorption structure

With the presence of Pt, the symmetry of CH_4 is reduced to C_{3v} symmetry [C–H_{ad}–Pt is the C_3 axis; see Fig. 1(a)] and the degeneracy of three bonding orbitals of CH_4, mainly composed of $2p_x$, $2p_y$, and $2p_z$ of C, is slightly broken into a_1 ($2p_z$) and e ($2p_x$ and $2p_y$) orbitals. The ground state is $^1A_1$, while the $1\,^1T_2$ state of CH_4 should become $^1A_1$ and ^1E states. The Hartree–Fock calculations verify that occupied orbitals of both CH_4 and Pt remain unperturbed, while Pt $6s$ virtual orbital mixes significantly with the CH_4 $3s$ Rydberg orbital and is largely perturbed. Note that the Rydberg orbital of CH_4 can easily interact with Pt due to its large spatial expanse. We carried out the SA-CASSCF(8/9) calculation for CH_4–Pt averaging the ground and three excited states, with eight valence orbitals of CH_4 and the (Pt $6s$)–(CH_4 $3s$) hybrid orbital in the active space. Pt $5d$ and C $1s$ were treated as frozen core orbitals during the CASSCF calculation. The calculated three excited states are well represented by a single electronic configuration in which one electron is excited from one of three CH bonding orbitals with a_1 or e symmetry to the (Pt $6s$)–(CH_4 $3s$) orbital. In this hybrid orbital, the weight of Pt $6s$ is large, so the transition to these excited states should cause electron transfer from CH_4 to Pt. Indeed, Mulliken net charges[24] on CH_4 in these states were calculated as 0.16–0.17. The excitation energy to the lowest excited state ($^1A_1$) was calculated as 9.50 eV, which is lower by 0.7 eV than that in the isolated CH_4. We confirmed that three C $3p$ Rydberg orbitals have a negligible effect on the excited states of interest.

Next, we carried out the SA-CASSCF(10/10) calculation by adding Pt $5d_{z^2}$ to the (8/9) active space, which can interact with CH bonding and antibonding orbitals composed of C $2p_z$ and H $1s$ orbitals (a_1 symmetry). The other Pt $5d$ orbitals with e symmetry were treated as frozen core orbitals, and the lowest five $^1A_1$ and two ^1E states were averaged with equal weight. The first two excited states

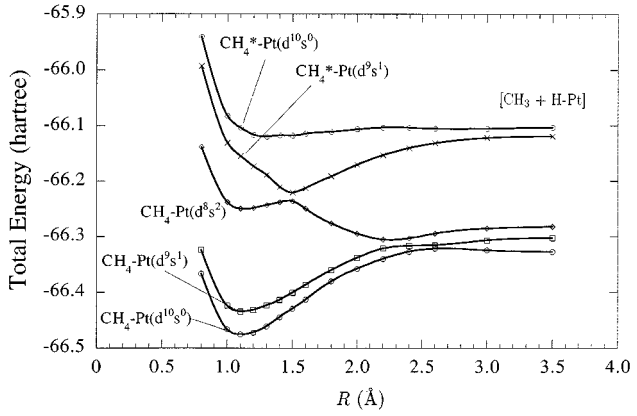

FIG. 3. Adiabatic potential energy curves of five $^1A_1$ states of CH_4–Pt as a function of the H_3C–HPt distance R calculated by the SA-CASSCF (10/10) method. The H_{ad}–Pt distance is fixed at 3.00 Å.

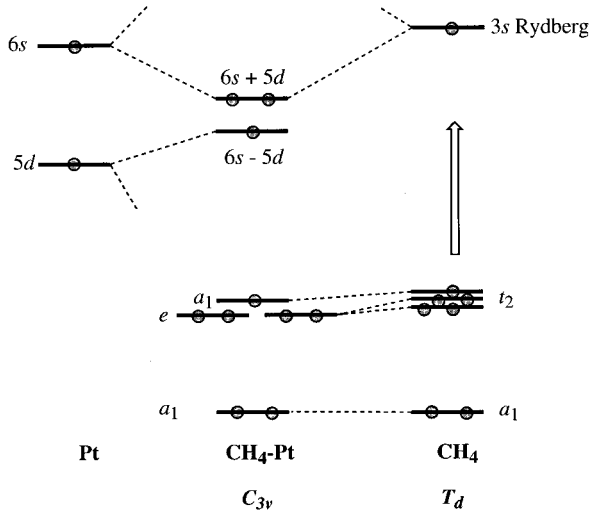

FIG. 4. Correlation diagram of significant orbitals of CH_4 3s Rydberg state and Pt.

($^1A_1$) are related to the excitation within a Pt atom: The electronic configuration of Pt in $X\ ^1A_1$, $2\ ^1A_1$, and $3\ ^1A_1$ can be written as $5d^{10}6s^0$, $5d^96s^1$, and $5d^86s^2$, respectively. Note that the corresponding electronic configurations of the isolated Pt atom are $5d^96s^1$, $5d^{10}6s^0$, and $5d^86s^2$, respectively. The lowest excited state due to the excitation from the CH bonding orbital is $4\ ^1A_1$, in which Pt has a configuration of $5d^96s^{1.5}$ that is close to $5d^96s^1$ (excited state) rather than $5d^{10}6s^0$ (ground state). The excitation energy to $4\ ^1A_1$ was calculated as 8.73 eV, which is lower than the corresponding value (9.50 eV) in the SA-CASSCF(8/9) calculation. This is because of a relaxation of $5d$ electrons in Pt: In the previous case, the Pt configurations are necessarily $5d^{10}$ in all electronic states while, in the present case, Pt $5d_{z^2}$ can be partially occupied. $5\ ^1A_1$ corresponds to this previously calculated excited state, in which the electron is excited from the CH bonding orbital and the configuration of the Pt atom is close to $5d^{10}6s^0$. In the excited states, due to the excitations from the CH_4 bonding orbitals ($4\ ^1A_1$, $5\ ^1A_1$, $1\ ^1E$, and $2\ ^1E$), the electron is transferred from CH_4 to Pt. Mulliken net charges[24] on CH_4 in these states were calculated as 0.48–0.72.

2. Dissociation into CH_3+HPt

The adiabatic potential energy curves for ground and excited states were calculated as a function of the H_3C–H_{ad} distance R by the SA-CASSCF(10/10) including the Pt $5d_{z^2}$ orbital in the active space. The H_{ad}–Pt distance is fixed at 3.00 Å. The energy curves with A_1 symmetry are shown in Fig. 3. The $4\ ^1A_1$ state is repulsive, so the transition to this state should lead to an immediate dissociation into CH_3 and H_{ad}–Pt in the ground state through three nonadiabatic transitions at $R=1.5$, 2.3, and 2.5 Å. On the Pt(111) surface, the reaction may proceed through a large number of nonadiabatic transitions. Figure 4 shows the correlation diagram of significant orbitals of the CH_4 3s Rydberg state and Pt. The CH a_1 bonding orbital is singly occupied, which becomes a $2p$ nonbonding orbital of CH_3 in the dissociation limit. The shifts of energy of CH bonding orbitals are relatively small. Pt $5d_{z^2}$ and 6s orbitals are strongly mixed through the interaction with the CH_4 3s Rydberg orbital, forming bonding and antibonding orbitals between H_{ad} and Pt at a large R. Because the electron of H_{ad} (and C) is partly transferred to Pt, H_{ad} becomes nearly protonlike and can be easily trapped into the Pt $5d$ orbital to make a chemical bond between H_{ad} 1s and Pt $5d_{z^2}$, while the CH_{ad} bond cleaves. In other words, an electron is donated from CH_4 3s to Pt 6s and backdonated from Pt $5d$ to a CH antibonding orbital (H_{ad} 1s). This donation–backdonation interaction can be invoked only through the Rydberg-type excited state of CH_4.

The $5\ ^1A_1$ state, which is also caused by the excitation from the CH bonding orbital, is repulsive and yields CH_3 in the ground state and H_{ad}–Pt in the excited state. The other excited states, related to the excitation within the Pt atom or the excitation from the CH e bonding orbitals, show energy minima around $R=1.1$ Å.

D. CH_4–Pt_4

1. Ground and excited states at the adsorption structure

Next, we discuss the CH_4–Pt_4 system in which the three neighboring Pt atoms on the second layer of the Pt(111) surface are added to the CH_4–Pt system [Fig. 1(a)]. The Pt atom which interacts directly with CH_4 is denoted as Pt_{ad}. In the same way as the CH_4–Pt system, we carried out SA-CASSCF calculations with (8/9) and (10/10) active spaces for CH_4–Pt_4. In the SA-CASSCF(10/10) calculation, the orbital composed mainly of Pt_{ad} $5d_{z^2}$ was included in the active space. In comparison with the CH_4–Pt system, the excitation energy of CH_4 decreases (8.73→8.25 eV), approaching the experimental value (6.43 eV). In the excited states due to the excitation from CH bonding orbitals, more than one electron is transferred from CH_4 to Pt, which is redistributed all over the Pt atoms. This is why the excitation energy becomes lower than that in CH_4–Pt. The difference

TABLE I. Leading configurations, excitation energy (eV), and oscillator strength (a.u.) for low-lying excited states of CH_4–Pt_4 calculated by the SA-CASSCF(12/11) method ($R=1.1$ Å).

State	Natural orbitals[a]					Coef.	Excitation energy	Oscillator strength
	CH a_1	CH e	$5d_{z^2}$ I	$5d_{z^2}$ II	$6s-6p$			
$X\ ^1A_1$	2	4	1	2	1	0.855	⋯	⋯
$2\ ^1A_1$	2	4	2	2	0	0.691	1.41	4.42×10^{-3}
	2	4	0	2	2	−0.462		
	2	4	1	1	2	0.405		
	2	4	1	2	1	−0.308		
$3\ ^1A_1$	2	4	2	2	0	0.689	1.81	2.66×10^{-2}
	2	4	0	2	2	0.418		
	2	4	1	1	2	−0.414		
	2	4	1	2	1	0.350		
$4\ ^1A_1$	2	4	2	1	1	0.931	5.50	6.33×10^{-2}
$5\ ^1A_1$	2	4	1	1	2	0.675	6.93	1.68×10^{-1}
	2	4	0	2	2	0.628		
$6\ ^1A_1$	1	4	1	2	2	0.958	9.01	1.32×10^{-2}
$1\ ^1E$	2	3	1	2	2	0.974	9.20	1.81×10^{-4}
$7\ ^1A_1$	1	4	2	2	1	0.964	10.52	1.19×10^{-2}

[a]CH a_1 and CH e denote CH bonding orbitals of a_1 and e symmetry, respectively; $5d_{z^2}$ I and $5d_{z^2}$ II denote Pt $5d_{z^2}$ related orbitals mixed with $5d$ orbitals of other Pt atoms; $6s-6p$ denotes (CH_4 $3s$)–(Pt_{ad} $6s,6p$) hybrid orbital.

between the SA-CASSCF(8/9) and SA-CASSCF(10/10) excitation energies becomes smaller than that in CH_4–Pt because Pt_{ad} has a configuration of $5d^96s^1$ in both the ground and the lowest excited state related to the excitation from the CH bonding orbital ($4\ ^1A_1$).

In the calculation of potential energy curves for CH_4–Pt_4 as a function of the H_3C–H_{ad} distance R, we first employed a SA-CASSCF(10/10) wave function like the CH_4–Pt system. Then, it proved that the $4\ ^1A_1$ state is repulsive in the region of $R\leqslant2.4$ Å, but the CASSCF calculation did not converge at $R\sim2.4$ Å. This is due to the insufficient active space; there are two orbitals related to Pt_{ad} $5d_{z^2}$, but only one (in which $5d_{z^2}$ has a larger contribution) was included in the active space. Thus, we carried out the SA-CASSCF(12/11) calculation, including the additional orbital of Pt_{ad} $5d_{z^2}$ character (which is delocalized over Pt_4) in the active space, and succeeded in getting convergences of the wave function in the range of $R=0.8$–5.0 Å. In this calculation, seven $^1A_1$ and one ^1E states are averaged with equal weight. The H_{ad}–Pt_{ad} distance is fixed at 3.00 Å determined for CH_4–Pt_7.

Before discussing the dissociation process into CH_3+HPt_4, we analyze results of SA-CASSCF(12/11) calculations at the adsorption structure ($R=1.1$ Å). Table I gives the leading configurations, excitation energy, and oscillator strength of the eight calculated states. The lowest excited state related to the excitation from the CH bonding orbital is $6\ ^1A_1$. The excitation energy to this state is calculated to be 9.01 eV, which is larger than the SA-CASSCF (10/10) values in CH_4–Pt and CH_4–Pt_4 systems. Figure 5 shows contour maps of significant natural orbitals given in Table I: CH a_1,e bonding orbitals, Pt_{ad} $5d_{z^2}$ related orbitals (I, II), and (CH_4 $3s$)–(Pt_{ad} $6s,6p$) hybrid orbital. The $5d_{z^2}$ II orbital is delocalized over Pt_4, which is not largely perturbed through the dissociation of H_3C–H. In Pt_{ad}, the strong hybrid of $5d_{z^2}$ and $6s$ is not observed while $6s$ mixes with $6p_z$. Atomic orbital populations and Mulliken net charges of CH_4 in the respective states are given in Table II. In the excited states due to the excitations from CH bonding orbitals ($6,7\ ^1A_1$ and $1\ ^1E$), 1.0–1.2 electrons are transferred from CH_4 to Pt_4, coinciding with the corresponding values in the SA-CASSCF(10/10) calculation. In $6\ ^1A_1$ [$(\mathrm{CH}\ a_1)^1(\mathrm{CH}\ e)^4$] and $1\ ^1E$ [$(\mathrm{CH}\ a_1)^2(\mathrm{CH}\ e)^3$], the transferred electron is distributed over four Pt atoms (0.28–0.30 per one Pt). On the other hand, in $7\ ^1A_1$, the electron from CH_4 is localized on Pt_{ad}, which has 0.816 excess electrons (the other three Pt atoms have 0.086 excess electrons). As another notable feature, the atomic orbital populations of the Pt atoms other than Pt_{ad} are almost independent of electronic states (i.e., $5d^{9.6}6s^{0.2-0.4}6p^{0.1}$).

2. Dissociation into CH_3+HPt_4

Figure 6 shows adiabatic potential energy curves of seven $^1A_1$ states calculated by the SA-CASSCF(12/11) method, in which Pt_{ad} configurations of the respective states are given in parentheses. There are two dissociation channels, $6\ ^1A_1$ and $7\ ^1A_1$, both of which are due to the excitations from the CH a_1 bonding orbital, but are different in the configurations of Pt_{ad}: the former is $5d^{9.1}6s^{1.1}$ while the latter is $5d^{9.9}6s^{0.8}$. The ground and other excited states due to excitations within Pt_4 or excitations from CH e bonding or-

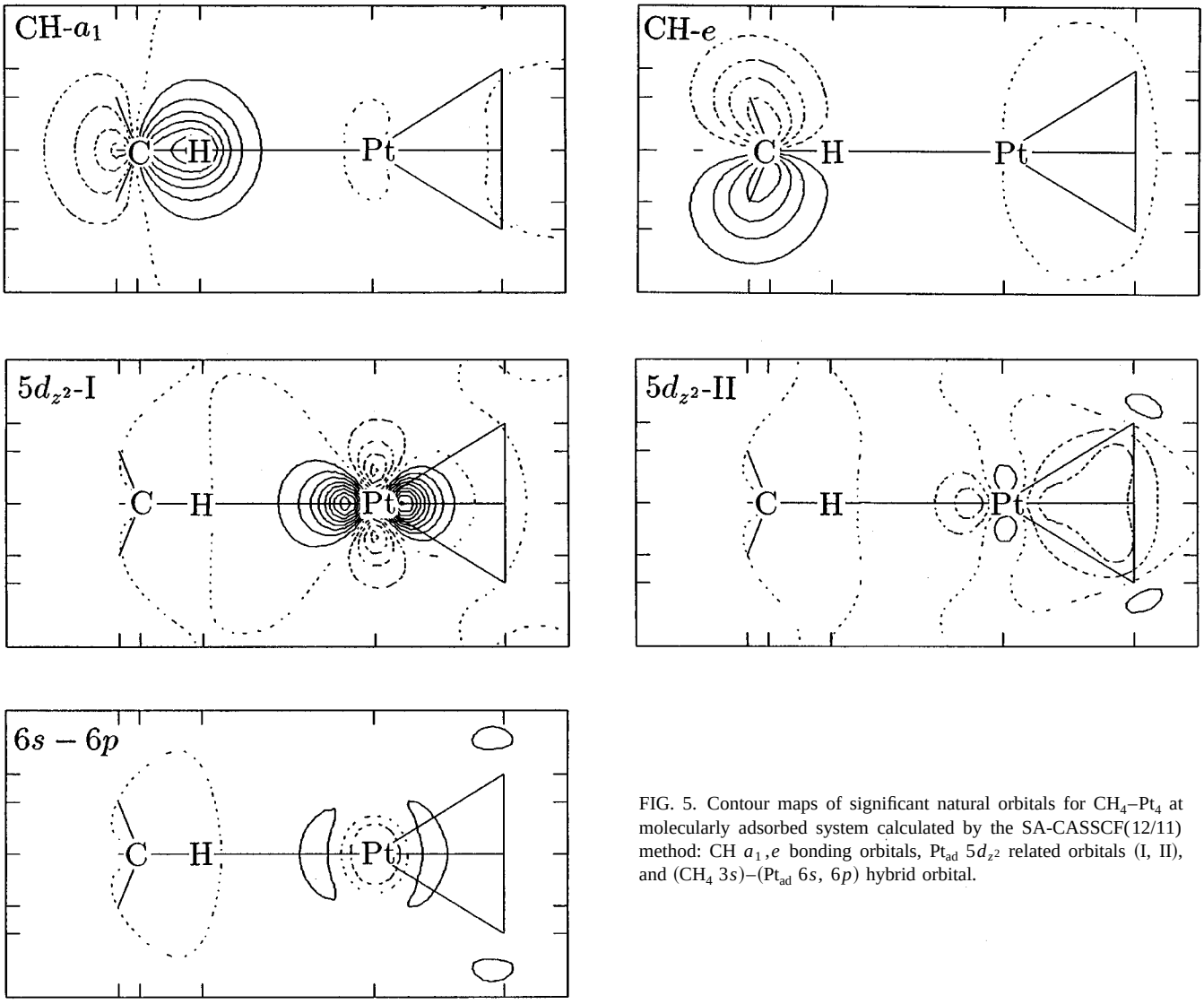

FIG. 5. Contour maps of significant natural orbitals for CH_4–Pt_4 at molecularly adsorbed system calculated by the SA-CASSCF(12/11) method: CH a_1, e bonding orbitals, Pt_{ad} $5d_{z^2}$ related orbitals (I, II), and (CH_4 $3s$)–(Pt_{ad} $6s$, $6p$) hybrid orbital.

bitals, have potential minima around $R=1.1$ Å, coinciding with the CH_4–Pt system. The $6\,^1A_1$ and $7\,^1A_1$ states lead to dissociations into CH_3 (ground state)+HPt_4 (ground state) through five nonadiabatic transitions at $R=1.35$, 1.5, 2.1, 2.3, and 3.2 Å, and CH_3 (ground state)+HPt_4 (excited state) through three nonadiabatic transitions at $R=1.3$, 1.6, and 1.9 Å, respectively. In all the states shown in Fig. 6, the electronic state of CH_3 becomes the ground state in the dissociation limit.

As CH_{ad} bond cleaves, a $H_{ad}Pt_{ad}$ bond is formed in the same way as the CH_4–Pt system. This bond is well localized, and the other Pt atoms on the second layer do not participate in this bond. This implies that the interaction between CH_4 and Pt_4 can be represented essentially using one Pt atom directly connected to H_{ad}, although the excitation energy depends on the size of the cluster because the electron transferred from CH_4 is distributed all over the Pt cluster.

E. CH_4–Pt_7

Next, we consider the CH_4–Pt_7 system in which all the neighboring Pt atoms on the first layer are included [Fig. 1(a)]. We carried out the SA-CASSCF(10/10) calculation, in which eight valence orbitals of CH_4 and two hybrid orbitals composed of CH_4 $3s$, Pt_{ad} $5d_{z^2}$, and Pt_{ad} $6s$ were included in the active space. In the ground state, $X\,^1A_1$, Pt_{ad} has the configuration of $5d^{9.0}6s^{0.5}6p^{0.4}$. The first two excited states ($^1A_1$) are due to the excitations within the Pt_7 cluster, in which the configurations of Pt_{ad} are $5d^{9.7}6s^{0.3}6p^{0.4}$ and $5d^{8.4}6s^{0.4}6p^{0.6}$, respectively. As to the excited states due to the excitations from the CH bonding orbitals, Pt_{ad} has the configuration of $5d^{9.0}6s^{0.6}6p^{0.4}$ in both $4\,^1A_1$ and $1\,^1E$ states, and the configuration of $5d^{9.7}6s^{0.5}6p^{0.4}$ in both $5\,^1A_1$ and $2\,^1E$ states. Note that the population of Pt_{ad} $6p$ is relatively large. The configurations of the surrounding six Pt atoms are not perturbed by transitions ($5d^{9.8}6s^{0.15}6p^{0.1}$) like the previous smaller system, and in addition, the configuration of Pt_{ad} also comes to be a bit indistinguishable among different states. This trend becomes more marked in a larger cluster system, as we see later. The excited states due to the excitations from CH bonding orbitals ($4\,^1A_1$, $5\,^1A_1$, $1\,^1E$, and $2\,^1E$) are a charge transfer type, in which CH_4 has a

TABLE II. Atomic orbital populations and Mulliken net charges (Ref. 24) for several electronic states of CH_4–Pt_4 calculated by the SA-CASSCF(12/11) method ($R=1.1$ Å).

State	Atom	s	p	d	Charge	Net charge of CH_4
$X\ ^1A_1$	Pt_{ad}	1.017	0.076	9.017	−0.111	0.192
	Pt_{other}[a]	0.394	0.111	9.522	−0.027	
	C	2.897	2.603	0.004	0.497	
	H_{ad}	0.848	0.059	0.000	0.093	
	H	1.123	0.010	0.000	−0.133	
$2\ ^1A_1$	Pt_{ad}	0.657	0.142	9.453	−0.252	0.097
	Pt_{other}	0.281	0.100	9.568	0.052	
	C	2.891	2.599	0.004	0.507	
	H_{ad}	0.964	0.057	0.000	−0.021	
	H	1.120	0.010	0.000	−0.130	
$3\ ^1A_1$	Pt_{ad}	0.439	0.169	9.513	−0.121	0.049
	Pt_{other}	0.244	0.100	9.633	0.024	
	C	2.888	2.596	0.004	0.512	
	H_{ad}	1.001	0.070	0.000	−0.075	
	H	1.119	0.010	0.000	−0.129	
$4\ ^1A_1$	Pt_{ad}	0.704	0.137	9.672	−0.513	0.100
	Pt_{other}	0.303	0.106	9.454	0.137	
	C	2.890	2.599	0.004	0.506	
	H_{ad}	0.936	0.068	0.000	−0.004	
	H	1.124	0.010	0.000	−0.134	
$5\ ^1A_1$	Pt_{ad}	1.176	0.080	8.349	0.395	0.221
	Pt_{other}	0.460	0.125	9.620	−0.205	
	C	2.896	2.593	0.005	0.507	
	H_{ad}	0.839	0.074	0.000	0.087	
	H	1.113	0.011	0.000	−0.124	
$6\ ^1A_1$	Pt_{ad}	1.119	0.073	9.093	−0.284	1.114
	Pt_{other}	0.466	0.131	9.681	−0.278	
	C	3.014	2.418	0.007	0.562	
	H_{ad}	0.349	0.105	0.000	0.545	
	H	0.986	0.010	0.000	0.996	
$1\ ^1E$	Pt_{ad}	1.151	0.071	9.089	−0.311	1.177
	Pt_{other}	0.474	0.131	9.683	−0.289	
	C	3.021	2.408	0.007	0.564	
	H_{ad}	0.658	0.096	0.000	0.247	
	H	0.864	0.014	0.000	0.122	
$7\ ^1A_1$	Pt_{ad}	0.792	0.142	9.882	−0.816	1.073
	Pt_{other}	0.317	0.102	9.667	−0.086	
	C	3.013	2.415	0.006	0.566	
	H_{ad}	0.444	0.077	0.000	0.478	
	H	0.980	0.105	0.000	0.009	

[a]Pt_{other} denotes Pt atoms other than Pt_{ad}.

positive charge (0.57–0.8). The excitation energy to $4\ ^1A_1$ was calculated as 6.80 eV.

Since the features of the excited states caused by the excitation from the CH bonding orbitals are basically the same as the previous cases, one can expect that the same reaction should occur (CH_4–$Pt_n+h\nu\rightarrow CH_3+H$–$Pt_n$) in the CH_4–Pt_7 system.

F. CH_4–Pt_{10}

In the largest system, CH_4–Pt_{10}, all the possible neighboring Pt atoms are included [Fig. 1(a)]. For these neighboring nine Pt atoms, smaller ($2s1p1d$) basis sets were used, as we mentioned. This imbalance of basis sets probably makes atomic orbital population of Pt atoms less reliable than previous cases.[24] The SA-CASSCF(10/10) calculation was carried out for the CH_4–Pt_{10} in the same way as the previous cases. The active space includes eight valence orbitals of CH_4 and two hybrid orbitals, composed of CH_4 $3s$ and two orbitals of Pt_{10}, which is mainly composed of Pt_{ad} $5d_{z^2}$ and Pt_{ad} $6p$ (although atomic orbitals of other Pt atoms have significant contributions). The population of Pt_{ad} $6p$ is larger than 1.0, while the other Pt atoms have 0.2–0.3 electrons in their respective $6p$ orbitals in both the ground and excited

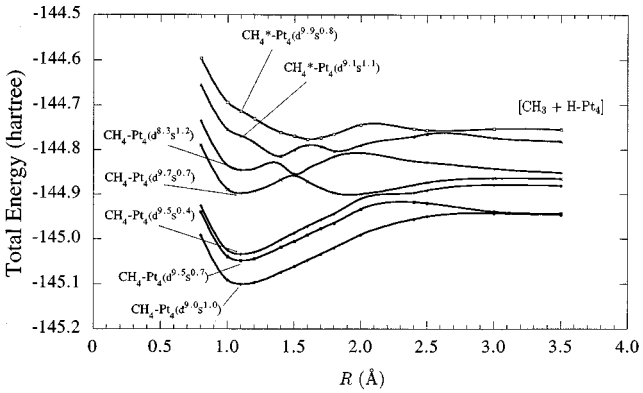

FIG. 6. Adiabatic potential energy curves of seven $^1A_1$ states of CH_4–Pt_4 as a function of the H_3C–HPt_4 distance R calculated by the SA-CASSCF (12/11) method. The H_{ad}–Pt_{ad} distance is fixed at 3.00 Å.

states.[24] Another remarkable feature is that Pt_{ad} has almost the similar electronic configuration of $5d^{9.1}6s^{0.47}6p^{1.1}$ in all the electronic states. Population analysis suggests that in the lowest excited states due to the excitation from the CH a_1 and e bonding orbitals, $4\,^1A_1$ and $1\,^1E$, the electron distribution to the surrounding Pt atoms is almost the same between the first layer and the second layer Pt atoms, while in $5\,^1A_1$ and $2\,^1E$, which are also due to the excitation from the CH bonding orbital, the electron is distributed mainly to the second layer Pt atoms.

The charge redistributions upon excitations from the ground state to the $4\,^1A_1$ and $5\,^1A_1$ states can easily be seen from the density difference maps given in Fig. 7. It is clear that the charge transfer occurs from the CH bonding orbital of CH_4 to Pt_n upon excitation. Figure 7 also indicates that, in both states, the transferred electrons spread out in the whole Pt_{10} cluster in both vertical and horizontal directions mainly through the $5d_{z^2}$ orbitals. In the $4\,^1A_1$, the charge delocalization is more significant in the horizontal direction (the first layer) rather than the vertical direction (the second layer), while in $5\,^1A_1$ it is more significant in the vertical direction rather than the horizontal direction.

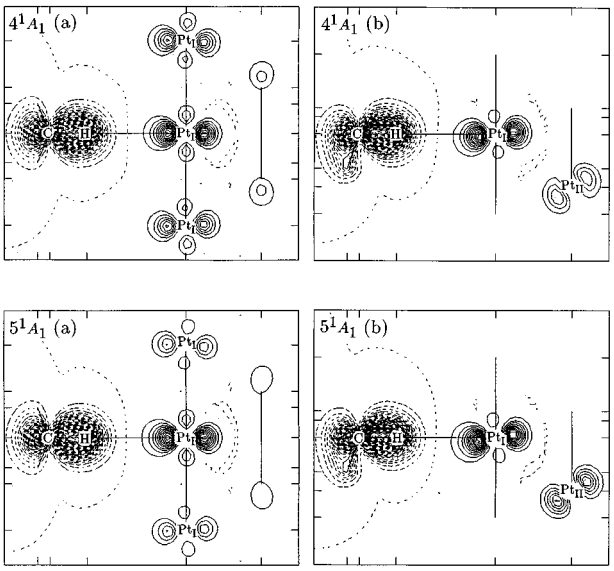

FIG. 7. The density difference maps for CH_4–Pt_{10} upon excitation to $4\,^1A_1$ and $5\,^1A_1$ in sections that include (a) C, H_{ad}, Pt_{ad}, and two more Pt atoms of the first layer (Pt_I) and (b) C, H_{ad}, Pt_{ad}, and one of the Pt atoms of the second layer (Pt_{II}). The density difference is calculated as $\rho_{\text{excited state}}-\rho_{\text{ground state}}$. The full lines and the broken lines denote the increase and the decrease of the charge density due to the transition from the ground state to the excited state, respectively.

The excitation energies of CH_4 in CH_4–Pt_n systems are summarized in Table III. It is observed that the excitation energy tends to decrease as a cluster becomes large, although the excitation energy in CH_4–Pt_{10} (7.76 eV) is a bit larger than that in CH_4–Pt_7 (6.80 eV). This may be due to the basis set deficiency. However, the effect of the surface may be sufficiently represented by the Pt_{10} cluster. As mentioned above, the excitation mechanism of the adsorbed molecule on the solid surface is classified into a direct or a surface-mediated excitation. Matsumoto *et al.*[7–9] suggested that direct excitation is more feasible in the CH_4/Pt(111) system, and that the Rydberg state of CH_4 mixes with the Pt surface electronic state, leading to a redshift of about 2 eV in the excitation energy. Our present study shows that the hybridization is actually invoked between a CH_4 $3s$ Rydberg state and Pt surface unoccupied states, and the resulting excited state has a Pt-like character rather than the Rydberg state of CH_4. Consequently, the transition to this state causes electron transfer from CH_4 to Pt, and a protonlike hydrogen atom easily forms a chemical bond with Pt. On the other hand, the excitations within the Pt_n cluster or from the CH e bonding orbitals do not cause the dissociation into CH_3 and H. These results clearly show that the photodissociation of CH_4 adsorbed on the Pt(111) surface should be triggered by the

TABLE III. SA-CASSCF excitation energy (eV) for a CH_4 $3s$ Rydberg state in CH_4–Pt_n ($n=0$, 1, 4, 7, 10).

Active space	CH_4	CH_4–Pt	CH_4–Pt_4	CH_4–Pt_7	CH_4–Pt_{10}
(8/9)	10.16	9.50	8.56	7.22	7.32
(10/10)	⋯	8.73	8.25	6.80	7.76

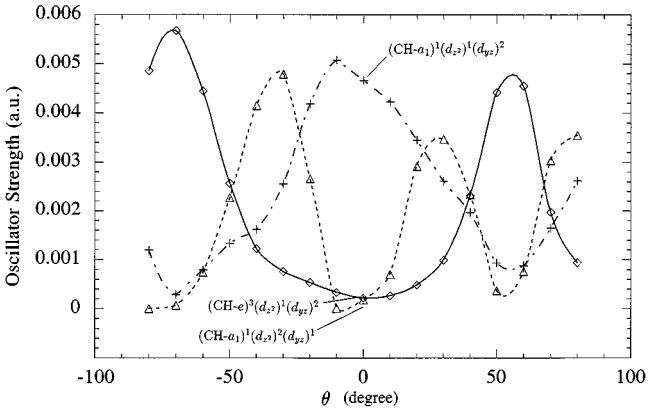

FIG. 8. Oscillator strengths as a function of Pt–C–H_{ad} bending angle θ. See also Fig. 9.

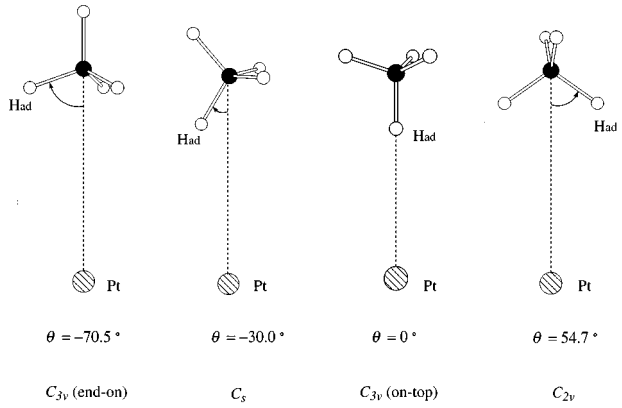

FIG. 9. CH_4–Pt structures corresponding to four peaks in Fig. 8.

direct excitation of CH_4. Moreover, our results suggest that the similar surface reaction leading to the dissociation can occur in the system that includes the molecule having a Rydberg state in relatively low energy region.

If one intends to study quantitatively such surface reactions accompanying the large charge transfer between the adsorbate and the surface, a larger cluster or the other adequate representation for a metal surface should be required. However, we believe the excitation mechanism of CH_4/Pt(111) with the relatively large shift of excitation energy despite the weak interaction in the ground state is essentially clarified in present study.

G. Effect of symmetry lowering

So far, we have discussed only C_{3v} symmetry adsorption structures. However, because of a small binding energy of CH_4 on Pt(111), this C_{3v} symmetry can be easily lost in a dynamical situation. Indeed, the adsorption structure of CH_4/Pt(111) has not been experimentally identified yet. Thus, it is meaningful to examine the effects of symmetry lowering of adsorption structures. Hence, we investigated the excited states due to excitations from CH bonding orbitals in CH_4–Pt system. The C_{3v} symmetry is broken into C_s symmetry structures in which the Pt atom is rotated around CH_4 with the C–Pt distance fixed at 4.1 Å. The excitation energies and the corresponding oscillator strengths were calculated as a function of a bending angle of $H_{ad}CPt$ (θ) by the SA-CASSCF(12/11) method; $\theta=-70.5°$, 0°, and 54.7° corresponds to C_{3v} (end-on), C_{3v} (on-top), and C_{2v} symmetry structures, respectively. Here, two Pt $5d$ orbitals of a' in C_s symmetry, $5d_{z^2}$ and $5d_{yz}$, were included in the active space, while the others remained in the frozen core.

Figure 8 shows variations of oscillator strengths for the three excited states due to excitations from CH bonding orbitals: $^1A_1$ with $(\mathrm{CH}\ a_1)^1(5d_{z^2})^1(5d_{yz})^2$; ^1E with $(\mathrm{CH}\ e)^3(5d_{z^2})^1(5d_{yz})^2$; ^1E with $(\mathrm{CH}\ a_1)^1(5d_{z^2})^2(5d_{yz})^1$. It is shown that the oscillator strengths vary largely during the rotation of the Pt atom, although the corresponding excitation energies are almost constant (as to the lowest state, the variation is ~0.6 eV). There are four notable peaks in oscillator strength (0.005–0.006 a.u.). The corresponding structures are shown in Fig. 9. At $\theta=0°$, the $^1A_1$ state, which leads to the dissociation into CH_3 and H as discussed in earlier subsections, has a relatively large oscillator strength. However, it decreases as Pt deviates from the C_3 axis. The two ^1E states have negligible oscillator strength at the C_{3v} (on-top) symmetry structure. However, at the C_{2v} and the C_{3v} (end-on) symmetry structures, the ^1E with $(\mathrm{CH}\ e)^3(5d_{z^2})^1(5d_{yz})^2$ shows large oscillator strengths. The ^1E with $(\mathrm{CH}\ a_1)^1(5d_{z^2})^2(5d_{yz})^1$ also shows a peak at $\theta\sim-30°$, which corresponds to the $^1A'$ state in C_s symmetry. In the C_{2v} and C_s structures shown in Fig. 9, Pt $5d_{z^2}$ and $5d_{yz}$ orbitals can have significant overlap with CH bonding and antibonding orbitals, and so, the cleaving CH bonds are located feasibly, but evidently the dissociation into CH_3 and H cannot occur keeping C_{2v} symmetry. In the ^1E having the peak at the C_s structure, the CH bonding orbital directed to Pt is singly occupied and the dissociation may take place. Thus, it can be said that the photodissociation of CH_4 can take place not only at a C_{3v} symmetry structure but also at a C_s symmetry structure.

IV. CONCLUSION

The photodissociation of CH_4 on the Pt(111) surface was studied using a cluster model with several sizes, focusing on the effect of Pt_n on the Rydberg-type $1\,^1T_2$ state of CH_4. It was shown that the first excited state of CH_4 (the $3s$ Rydberg state) interacts strongly with the Pt unoccupied $6s$ or $6p$ orbitals, resulting in the charge transfer state, which lies 6.80–9.01 eV above the ground state. The excitation energy becomes lower by 1.15–3.25 eV than that in an isolated CH_4, which is in good agreement with the experiments. The adiabatic potential energy curves were calculated as a function of H_3C–H distance in CH_4–Pt and CH_4–Pt_4 systems, and it was found that transitions to these charge transfer states lead to immediate dissociations into a CH_3 radical and H–Pt(111). Similar results were obtained in larger cluster systems. The photoexcitation, followed by the dissociation, was explained by the interaction among CH_4 $3s$ Rydberg, Pt unoccupied $6s$ (or $6p$), and Pt $5d$ orbitals. The excitation energy largely depends on the cluster size because the elec-

tron redistribution over the surrounding metal atoms plays an important role to stabilize the corresponding charge transfer state.

The oscillator strengths of several excited states were also calculated with the reduction of C_{3v} symmetry of the adsorption structure to C_s symmetry, by rotating CH_4 relative to the Pt surface. The results indicate that the photodissociation of CH_4 into CH_3 and H can take place also at the C_s symmetry structures.

Our present study suggests the possibility that the similar reaction should occur in the system including the molecule, which has low-lying Rydberg states leading to the dissociation.

ACKNOWLEDGMENTS

The present research is supported in part by a grant-in-aid for scientific research from the Ministry of Education, Science and Culture of Japan and by a grant from New Energy and Industrial Technology Development Organization (NEDO). One of the authors (K.H.) is grateful for a grant from the Kawasaki Steel 21st Century Foundation. Orbital contour maps and differential density maps were plotted using the GAMESS program.[25]

[1] X.-L. Zhou, X.-Y. Zhu, and J. M. White, Surf. Sci. Rep. **13**, 73 (1991).
[2] H. Nakatsuji, H. Morita, H. Nakai, Y. Murata, and K. Fukutani, J. Chem. Phys. **104**, 714 (1996).
[3] H. Nakatsuji and K. Hirao, J. Chem. Phys. **68**, 2035 (1978); H. Nakatsuji, Chem. Phys. Lett. **59**, 362 (1978); Chem. Phys. **75**, 425 (1983); K. Hirao, J. Chem. Phys. **79**, 5000 (1983); **95**, 3589 (1991).
[4] H. Nakatsuji, H. Nakai, and Y. Fukunishi, J. Chem. Phys. **95**, 640 (1991).
[5] Z. C. Ying and W. Ho, J. Chem. Phys. **93**, 9077 (1990); **94**, 5701 (1991); S. K. So and W. Ho, *ibid*. **95**, 656 (1991).
[6] X.-Y. Zhu and J. M. White, J. Chem. Phys. **94**, 1555 (1991).
[7] Y. A. Gruzdkov, K. Watanabe, K. Sawabe, and Y. Matsumoto, Chem. Phys. Lett. **227**, 243 (1994).
[8] K. Watanabe, K. Sawabe, and Y. Matsumoto, Phys. Rev. Lett. **76**, 1751 (1996).
[9] Y. Matsumoto, Y. A. Gruzdkov, K. Watanabe, and K. Sawabe, J. Chem. Phys. **105**, 4775 (1996).
[10] L. C. Lee and C. C. Chang, J. Chem. Phys. **78**, 688 (1983).
[11] G. Herzberg, *Electron Spectra and Electronic Structure of Polyatomic Molecules* (Van Nostrand, New York, 1966), pp. 526–528.
[12] C. Lee, W. Yang, and R. G. Parr, Phys. Rev. B **37**, 785 (1988).
[13] A. D. Becke, Phys. Rev. A **38**, 3098 (1988).
[14] B. Miechlich, A. Savin, H. Stoll, and H. Preuss, Chem. Phys. Lett. **157**, 200 (1989).
[15] B. O. Roos, P. Bruna, S. D. Peyerimhoff, and R. Shepard, *Ab Initio Quantum Chemistry II*, edited by K. P. Lawley [Adv. Chem. Phys. **67**, 63 (1987)].
[16] J. Yoshinobu, H. Ogasawara, and M. Kawai, Phys. Rev. Lett. **75**, 2176 (1995).
[17] M. J. Frisch, G. W. Trucks, H. B. Schlegel, P. M. W. Gill, B. G. Johnson, M. A. Robb, J. R. Cheeseman, T. Keith, G. A. Petersson, J. A. Montgomery, K. Raghavachari, M. A. Al-Laham, V. G. Zakrzewski, J. V. Ortiz, J. B. Foresman, J. Cioslowski, B. B. Stefanov, A. Nanayakkara, M. Challacombe, C. Y. Peng, P. Y. Ayala, W. Chen, M. W. Wong, J. L. Andres, E. S. Replogle, R. Gomperts, R. L. Martin, D. J. Fox, J. S. Binkley, D. J. Defrees, J. Baker, J. P. Stewart, M. Head-Gordon, C. Gonzalez, and J. A. Pople, GAUSSIAN 94, Revision D.1, Gaussian, Inc., Pittsburgh, PA, 1995.
[18] L. E. Sutton, *Tables of Interatomic Distances and Configuration in Molecules and Ions* (Royal Society of Chemistry, London, 1965).
[19] MOLPRO is a package of *ab initio* programs written by H.-J. Werner and P. J. Knowles, with contributions from J. Almlöf, R. D. Amos, M. J. O. Deggan, S. T. Elbert, C. Hampel, W. Meyer, K. Peterson, R. Pitzer, A. J. Stone, and P. R. Taylor. See also: H.-J. Werner and P. J. Knowles, J. Chem. Phys. **82**, 5053 (1985); P. J. Knowles and H.-J. Werner, Chem. Phys. Lett. **115**, 259 (1985).
[20] D. E. Woon and T. H. Dunning, Jr., J. Chem. Phys. **100**, 2975 (1989); **103**, 4572 (1995); T. H. Dunning, Jr., *ibid*. **90**, 1007 (1989).
[21] P. J. Hay and W. R. Wadt, J. Chem. Phys. **82**, 270 (1985).
[22] S. Karplus and R. Bersohn, J. Chem. Phys. **51**, 2040 (1969).
[23] M. S. Gordon and J. W. Caldwell, J. Chem. Phys. **70**, 5503 (1979).
[24] Mulliken net charges and orbital populations are notoriously ambiguous particularly for excited states in which diffuse orbitals are used; while Pt $5d$ populations are probably reasonable, Pt $6s$, $6p$ and C $3s$ populations are only a guide as are the net charges, etc., in the excited states.
[25] M. W. Schmidt *et al.*, J. Comp. Chem. **14**, 1347 (1993).